QED-Net: Quantum Emotional Dynamics Synthesis Network for Sentiment Analysis in Medical IoT

Journal:	*IEEE Transactions on Computational Social Systems*
Manuscript ID	TCSS-2025-02-0236
Manuscript Type:	Special Issue on Emotion AI and Sentiment Analysis in Social Systems
Date Submitted by the Author:	08-Feb-2025
Complete List of Authors:	Awan, Kamran Ahmad; University of Haripur, Department of Information Technology Uddin, Mueen; University of Doha for Science & Technology Alanazi, Meshari Huwaytim; Northern Border University College of Science Anwar, Muhammad Shahid; Gachon University Javaid, Nadeem; King Saud University College of Computer and Information Sciences Cheng, Xiaochun; Swansea University
Keywords:	Medical Internet of Things, Quantum Computing, Emotion Dynamics, Sentiment Analysis, Graph Modeling

QED-Net: Quantum Emotional Dynamics Synthesis Network for Sentiment Analysis in Medical IoT

Kamran Ahmad Awan, *Member, IEEE,* Mueen Uddin, *Senior Member, IEEE,*
Meshari Huwaytim Alanazi, *Member, IEEE,* Muhammad Shahid Anwar, *Member, IEEE,*
Khursheed Aurangzeb, *Member, IEEE,* and Xiaochun Cheng, *Senior Member, IEEE*

***Abstract*—The increasing reliance on IoMT systems highlights the need for efficient sentiment analysis, emotion tracking, and multimodal data fusion to enable real-time decision making in dynamic environments. Existing frameworks struggle with integrating diverse data modalities and managing temporal complexities in emotional and behavioral patterns. This study aims to address these gaps by proposing QED-Net, a quantum-inspired deep learning framework designed to improve IoMT applications. The framework introduces novel modules, including Quantum-Driven Sentiment Amplification (QSA) for precision in sentiment analysis, the Temporal Emotion Evolution Graph (TEEG) for tracking dynamic emotional transitions, and the Hyper-Dimensional Quantum Tensor Fusion (HD-QTF) for robust multimodal data integration. In addition, the Emotion-to-Medical Ontology Encoder (EMOE) maps emotional states to actionable medical insights in real time. The simulation results demonstrate the superiority of QED-Net, achieving 93. 2% sentiment precision, 92. 3% emotion tracking precision, and 91. 6% multimodal fusion robustness, which confirms its potential for real-world IoMT applications.**

***Index Terms*—Medical Internet of Things, Quantum Computing, Emotion Dynamics, Sentiment Analysis, Graph Modeling.**

I. Introduction

THE study of emotion detection and sentiment analysis has advanced significantly, driven by the growing use of machine learning and artificial intelligence [1]–[3]. These technologies enable systems to interpret human emotions from text, speech, facial expressions, and physiological signals. Applications range from social interaction analysis to medical diagnostics, where understanding emotional states can provide valuable information on mental and physical well-being [4]. Similarly, the Internet of Medical Things (IoMT) has gained prominence for its role in integrating wearable devices, sensors, and communication networks to deliver real-time healthcare solutions [5]. Current emotion recognition systems often fail to handle multimodal data effectively, particularly when they involve diverse sources such as EEG signals, facial expressions, or textual input [6], [7]. Similarly, sentiment analysis models frequently misinterpret nuanced emotions, such as sarcasm or blended emotional states, reducing their reliability in practical applications [8].

The motivation for this research lies in the need for an approach that addresses these limitations and bridges the gap between theory and application. The inability of existing models to process complex multimodal data or operate efficiently in IoMT scenarios presents a compelling problem statement [9]. The primary objective of this study is to design a novel framework that can accurately detect, interpret, and use emotional and sentiment data in real-time medical settings [10]. The proposed Quantum Emotional Dynamics Synthesis Network (QED-Net) introduces a framework to address the challenges in emotion detection and sentiment analysis. QED-Net operates on a foundation of quantum-inspired principles, modeling emotions as dynamic wave functions through the Emotion Particle Wave Function (EPWF). It employs Hyper-Dimensional Quantum Tensor Fusion (HD-QTF) for multimodal data integration, preserving the integrity and correlation of diverse modalities such as EEG, speech, and facial expressions. Additionally, the Temporal Emotion Evolution Graph (TEEG) ensures time-sensitive modeling of emotional patterns. The model is also supported by a real-time emotional behavior feedback loop (REFL), which introduces adaptive interventions within IoMT systems. The key contributions of this study can be summarized as:

1) Quantum-inspired mechanism that models emotional states as wave functions, capturing both intensity and superposition, enabling the representation of blended emotions that are unachievable by existing approaches.
2) Novel data integration framework that utilizes quantum tensor mathematics to maintain hierarchical and intrinsic correlations across multi-modal inputs.
3) Graph-based modeling paradigm that tracks emotion progression over time, capturing gradients and recurrent patterns to predict future emotional states.

The structure of this article can be summarized as follows:

Kamran Ahmad Awan is with the Department of Information Technology, The University of Haripur, Khyber Pakhtunkhwa, Pakistan e-mail: (kamranawan.2955@gmail.com)

Mueen Uddin is with the College of Computing and IT, University of Doha for Science and Technology, Doha, Qatar e-mail: (mueen.malik@ieee.org)

Meshari Huwaytim Alanazi is with the Computer Science Department, College of Sciences, Northern Border University, Arar, Saudi Arabia e-mail: (meshari.alanazi@nbu.edu.sa)

Muhammad Shahid Anwar is with the Department of AI and Software Gachon University Seongnam-si, 13120, South Korea e-mail: (shahidanwar786@gachon.ac.kr)

Khursheed Aurangzeb is with the Department of Computer Engineering, College of Computer and Information Sciences, King Saud University, P. O. Box 51178, Riyadh 11543, Saudi Arabia e-mail: (kaurangzeb@ksu.edu.sa)

Xiaochun Cheng is with The Computer Science Department, Bay Campus Fabian Way, Swansea University, Swansea, SA1 8EN Wales, UK e-mail (xiaochun.cheng@swansea.ac.uk)

Corresponding author is Kamran Ahmad Awan (kamranawan.2955@gmail.com) and co-corresponding author is Muhammad Shahid Anwar (shahidanwar786@gachon.ac.kr)

Section II explores existing research. *Section III* details the proposed QED-Net approach. *Section IV* presents the simulation environment and evaluates the performance of the model using various metrics. Finally, *Section VI* concludes the article.

II. Background Research Analysis

The domain of sentiment analysis in IoMT and healthcare systems has seen significant advancements, driven by diverse methodologies and frameworks. Adversarial learning has shown potential to improve the robustness of sentiment analysis models, especially when dealing with noisy or perturbed data in IoMT systems, as shown in [11]. Similarly, the application of recurrent neural networks, particularly Long Short-Term Memory (LSTM) networks, has been effective in analyzing multimodal data, such as online educational content within the IoT framework [12]. In healthcare-specific applications, convolutional networks combined with knowledge graphs have enabled enhanced drug recommendation systems by integrating user sentiments and drug interactions [13]. In addition, cutting-edge methods for sentiment-based pain detection in smart healthcare frameworks continue to refine patient monitoring systems [14].

Various machine learning frameworks have addressed domain-specific challenges in sentiment analysis. For example, models that integrate Word2Vec embeddings with boosting algorithms have improved the precision of drug recommendation systems by emphasizing semantic relationships [15]. Efforts in the domain of health diagnostics, such as analyzing sentiments related to diabetes using classification models, underscore the necessity of extracting actionable insights from patient narratives [16]. Sentiment-guided approaches to medical image classification have highlighted the relevance of linguistic cues in augmenting non-textual data analysis [17]. Furthermore, facial sentiment analysis using deep convolutional neural networks has achieved notable precision in identifying human emotions, particularly when semantic feature extraction techniques are employed [18]. Finally, semi-supervised methods for biomedical sentiment analysis have emerged as a promising direction, leveraging limited labeled data for health insights based on social networks [19].

The proposed approach addresses limitations inherent in existing methodologies by introducing novel components. Traditional models struggle to represent complex emotional states, accurately fuse multimodal data, and adapt to dynamic real-time IoMT environments. These gaps are mitigated through the EPWF, which captures blended emotions; HD-QTF, ensuring robust multimodal integration; and the TEEG, enabling predictive emotional modeling (see Table I).

III. Proposed QED-Net Approach

The QED-Net introduces a framework that redefines emotion and sentiment analysis through novel quantum-inspired methodologies. By integrating EPWF, HD-QTF, and TEEG, the model achieves advanced emotional representation, robust multimodal fusion, and predictive temporal modeling.

TABLE I
Analysis of Limitations and Their Addressal in the Proposed QED-Net Approach

Identified Limitation	Addressed by Proposed Approach
Inability to represent complex emotional states	Emotion Particle Wave Function (EPWF) for blended emotion representation
Limited effectiveness in multimodal data fusion	Hyper-Dimensional Quantum Tensor Fusion (HD-QTF) for robust data integration
Challenges in modeling time-sensitive emotional dynamics	Temporal Emotion Evolution Graph (TEEG) for predictive and dynamic emotional modeling
Difficulty in adapting to real-time IoMT constraints	Real-Time Emotion-Behavior Feedback Loop (REFL) for adaptive interventions

A. Workflow of QED-Net

The workflow begins with the EPWF, where emotional states are modeled as quantum-inspired wave functions, encapsulating both intensity (amplitude) and dynamic transitions (frequency). Subsequently, the QSA module refines sentiment signals employing entanglement-based mechanisms to dynamically amplify or suppress contextually significant features.

The temporal dynamics of emotions are captured and modeled by the TEEG. This component employs graph-based structures to represent emotion trajectories over time, incorporating gradients of change and recurrent emotional patterns. The EMOE bridges emotional states with medical data by mapping sentiments to physiological signals, thus generating a structured ontology. For data integration, the HD-QTF layer processes multi-modal inputs simultaneously, ensuring the preservation of intrinsic correlations and hierarchical relationships between data modalities. This fusion mechanism enables robust and real-time analysis, critical for IoMT's computational constraints. Finally, the REFL provides adaptive feedback based on detected emotions and predicted behaviors. This loop enhances the interactivity of the IoMT system by offering actionable interventions, thereby transforming passive monitoring into a dynamic and responsive process. The comprehensive workflow of the proposed QED-Net framework is illustrated in Figure 1, highlighting its modular design for emotion detection and sentiment analysis within IoMT systems.

B. Emotion Particle Wave Function (EPWF)

The EPWF introduces a novel mathematical framework to model complex and mixed emotional states using quantum-inspired principles. By incorporating amplitude to represent emotion intensity and frequency to encode dynamic emotional transitions, EPWF achieves an advanced representation of emotional complexities beyond conventional models.

$$\Psi(t,x) = A(t)\sin\big(\omega(t)x + \phi(t)\big) \tag{1}$$

The wave function $\Psi(t,x)$ in (1) defines emotional states as a function of time t and spatial variable x, with amplitude

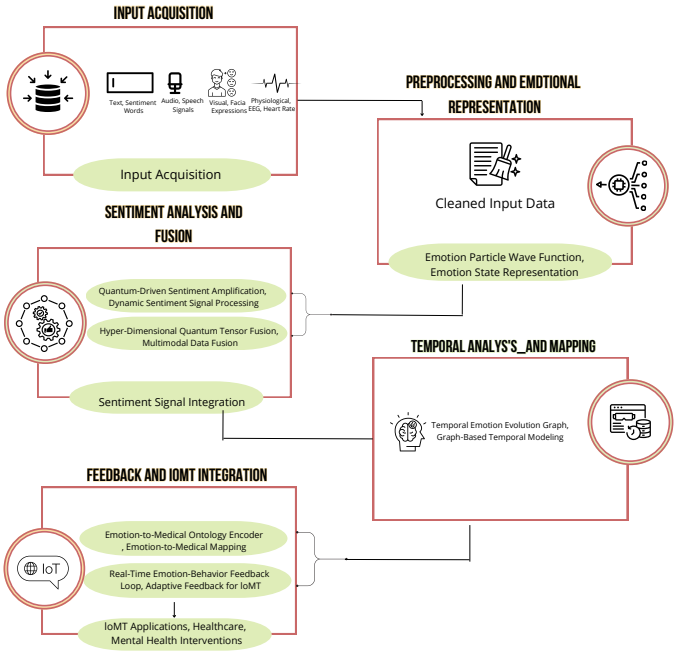

Fig. 1. Workflow of the QED-Net Framework: QED-Net integrates quantum-inspired modules for IoMT, modeling emotions as $\Psi(t,x) = A(t)\sin(\omega(t)x + \phi(t))$ with $A(t) = \exp\left(-\frac{t^2}{2\sigma^2}\right)$ and $\omega(t)$. Fusion uses $T = \bigotimes_{k=1}^{n} M_k$, with temporal modeling via $G_{t+1} = (V_t + \Delta V, E_t + \Delta E)$ and ontology mapping through $f(e_i, s_j) = \exp\left(-\alpha \cdot ||\phi(e_i) - \psi(s_j)||_2^2\right)$.

$A(t)$ and phase evolution $\phi(t)$ controlling the intensity and dynamics.

$$A(t) = \exp\left(-\frac{t^2}{2\sigma^2}\right) \tag{2}$$

$$\omega(t) = \omega_0 + \int_0^t \frac{\partial \Omega(u)}{\partial u}\, du \tag{3}$$

The amplitude $A(t)$ in (2) describes the emotional intensity, while the frequency $\omega(t)$ in (3) evolves based on temporal modulation.

$$\phi(t) = \phi_0 + \alpha \int_0^t \Psi'(t,x)\, dt \tag{4}$$

$$\Omega(u) = \beta \cos\left(\gamma u^2\right) \tag{5}$$

$$\Psi'(t,x) = \frac{\partial \Psi(t,x)}{\partial t} \tag{6}$$

The phase $\phi(t)$ in (4) integrates the wave derivative $\Psi'(t,x)$, enabling dynamic adjustments influenced by frequency modulation $\Omega(u)$ in (5). The derivatives in (6) provide the foundation for analyzing emotional transitions.

$$\Psi_k(t,x) = \sum_{i=1}^{n} A_i(t)\sin\left(\omega_i(t)x + \phi_i(t)\right) \tag{7}$$

Equations (7) extend the single emotional state $\Psi(t,x)$ into a multi-dimensional construct, where $\Psi_k(t,x)$ models multiple emotions.

$$\Phi(t) = \prod_{i=1}^{n} \cos\left(\psi_i(t)\right) \tag{8}$$

$$\psi_i(t) = \int_0^t \Psi_i'(t,x)\, dt \tag{9}$$

Blended emotional states are represented by the phase $\Phi(t)$ in (8), constructed using the derivatives $\psi_i(t)$ from (9).

$$A_{\text{blend}}(t) = \sqrt{\sum_{i=1}^{n} A_i^2(t)} \tag{10}$$

$$\Psi_{\text{blend}}(t,x) = A_{\text{blend}}(t)\sin\left(\omega_{\text{blend}}(t)x + \phi_{\text{blend}}(t)\right) \tag{11}$$

The blended amplitude $A_{\text{blend}}(t)$ in (10) and the corresponding wave function $\Psi_{\text{blend}}(t,x)$ in (11) allow seamless synthesis of complex emotional states.

$$\omega_{\text{blend}}(t) = \frac{1}{n}\sum_{i=1}^{n} \omega_i(t) \tag{12}$$

The frequency $\omega_{\text{blend}}(t)$ in (12) averages over multiple states, ensuring consistency across modalities.

$$\Psi_{\text{super}}(t,x) = \sum_{k=1}^{m} c_k \Psi_k(t,x) \tag{13}$$

Superposition of emotional states is achieved in (13) by combining multiple states $\Psi_k(t,x)$ weighted by c_k.

$$c_k = \frac{\exp(-\lambda_k t)}{\sum_{k=1}^{m}\exp(-\lambda_k t)} \tag{14}$$

$$\mathcal{H}(\Psi_{\text{super}}) = -\sum_{k=1}^{m} c_k \log(c_k) \tag{15}$$

The weights c_k in (14) are dynamically adjusted, and the entropy $\mathcal{H}(\Psi_{\text{super}})$ in (15) quantifies the complexity of the emotional distribution.

$$\Psi_{\text{adapt}}(t,x) = \Psi_{\text{super}}(t,x) + \delta(t,x) \tag{16}$$

$$\delta(t,x) = \epsilon\cos\left(\eta t + \kappa x\right) \tag{17}$$

Real-time adaptability is introduced via the perturbation $\delta(t,x)$ in (16) and (17), allowing dynamic adjustments to emotional states.

C. Quantum-Driven Sentiment Amplification (QSA)

The QSA module introduces a quantum-inspired mechanism to adaptively amplify or suppress sentiment signals utilizing entanglement principles. This process dynamically links contextual and multimodal input, optimizing sentiment representation through enhanced accuracy and interpretability.

$$S(t,x) = \sum_{i=1}^{n} c_i \psi_i(t,x) \tag{18}$$

$$c_i = \frac{\exp(-\lambda_i x)}{\sum_{j=1}^{n} \exp(-\lambda_j x)} \tag{19}$$

$$\psi_i(t,x) = A_i(t) \sin\big(\omega_i(t)x + \phi_i(t)\big) \tag{20}$$

$$\Delta S(t) = \int_0^t \frac{\partial S(t,x)}{\partial t}\, dt \tag{21}$$

$$\mathcal{Q}(S) = \sum_{i=1}^{n} \big| c_i \cdot \psi_i(t,x) \big|^2 \tag{22}$$

Equation (18) models sentiment signals $S(t,x)$ as a superposition of contextual inputs $\psi_i(t,x)$, with weights c_i determined dynamically using (19). Each input $\psi_i(t,x)$ is represented as a quantum wave function in (20), incorporating amplitude, frequency, and phase information. The change in sentiment signal $\Delta S(t)$ over time is calculated using (21), while the quantum amplification $\mathcal{Q}(S)$ in (22) quantifies the entangled contributions of all inputs. Further refinement is achieved through contextual dependencies and their corresponding impact on sentiment scores.

$$\mathcal{H}(S) = -\sum_{i=1}^{n} c_i \log(c_i) \tag{23}$$

$$\mathcal{A}(t,x) = \alpha \sum_{i=1}^{n} \big(\psi_i(t,x) - \bar{\psi}(t,x)\big)^2 \tag{24}$$

$$\bar{\psi}(t,x) = \frac{1}{n} \sum_{i=1}^{n} \psi_i(t,x) \tag{25}$$

$$\mathcal{F}(t) = \int_0^t \mathcal{A}(t,x)\, dx \tag{26}$$

Equation (23) measures the entropy of sentiment signals, providing insights into their interpretability. The variance $\mathcal{A}(t,x)$ in (24) quantifies the deviation of individual sentiment signals from their mean $\bar{\psi}(t,x)$, calculated in (25). The signal fidelity $\mathcal{F}(t)$ in (26) ensures consistency and reliability across dynamic inputs. Finally, the entangled sentiment representation is fine-tuned for multimodal fusion.

$$S_{\text{fused}}(t,x) = \sum_{k=1}^{m} \mathcal{Q}(S_k) \cdot W_k \tag{27}$$

$$W_k = \frac{1}{Z} \exp\big(-\mu_k S_k\big) \tag{28}$$

$$Z = \sum_{k=1}^{m} \exp\big(-\mu_k S_k\big) \tag{29}$$

$$\mathcal{L}(t) = \sum_{k=1}^{m} \big| S_{\text{fused}}(t,x) - S_k(t,x) \big|^2 \tag{30}$$

Equation (27) defines the fused sentiment signal $S_{\text{fused}}(t,x)$ as a weighted combination of amplified signals, with weights W_k determined through (28) and normalized using (29). The loss function $\mathcal{L}(t)$ in (30) optimizes the fidelity and accuracy of the fused sentiment representation, ensuring alignment with contextual and multimodal inputs.

Algorithm 1: Temporal Emotion Evolution Graph (TEEG)

Input: Initial graph $G_t = (V_t, E_t)$ at time t, temporal increment Δt, coefficients κ, λ
Output: Updated graph G_{t+1}, consistency loss $\mathcal{C}(t)$

Initialization: Set V_t, E_t for initial graph G_t;
while *time* $t \leq T$ **do**
  `// Update vertices and edges based on temporal gradients`
  Compute ΔV using (39);
  Compute ΔE using (40);
  Update graph: $G_{t+1} = \mathcal{T}(G_t, \Delta t)$ using (37);
  `// Recurrent feedback for loop consistency`
  Compute vertex loss $\mathcal{L}(t)$ using (41);
  Compute edge loss $\mathcal{R}(G_t)$ using (42);
  Calculate combined loss $\mathcal{C}(t) = \mathcal{L}(t) + \mathcal{R}(G_t)$ using (43);
  `// Adjust vertices and edges dynamically`
  Update $v_i(t)$ and $e_{ij}(t)$ based on feedback;
return G_{t+1}, $\mathcal{C}(t)$

D. Temporal Emotion Evolution Graph (TEEG)

The TEEG introduces a novel mathematical framework to model the dynamic progression of emotions over time. As described in Algorithm 1, the TEEG uses temporal gradients and recurrent feedback to dynamically update the graph structure.

By incorporating gradients, temporal dependencies, and recurrent loops, TEEG provides a structured and interpretable representation of emotional states, surpassing traditional methods in capturing time-sensitive patterns.

$$G_t = (V_t, E_t) \tag{31}$$

$$V_t = \{v_i(t) \,|\, i = 1, \ldots, N\} \tag{32}$$

$$E_t = \{e_{ij}(t) = f(v_i(t), v_j(t)) \,|\, i,j \in V_t\} \tag{33}$$

$$v_i(t) = \Psi_i(t) + \alpha \frac{\partial \Psi_i(t)}{\partial t} \tag{34}$$

$$e_{ij}(t) = \beta \cdot \cos\big(\gamma \cdot d_{ij}(t)\big) \tag{35}$$

$$d_{ij}(t) = ||v_i(t) - v_j(t)||_2 \tag{36}$$

In (31), the graph G_t represents the emotional state at time t with vertex set V_t and edge set E_t. Each vertex $v_i(t)$ in (32) corresponds to an individual emotional state, incorporating temporal changes as shown in (34). The edge $e_{ij}(t)$ in (33) quantifies the relationship between emotional states based on a weighted cosine function of their distance $d_{ij}(t)$, defined in (36). To capture temporal dynamics, TEEG evolves through successive states using graph transformations.

$$G_{t+1} = \mathcal{T}(G_t, \Delta t) \tag{37}$$

$$\mathcal{T}(G_t, \Delta t) = (V_t + \Delta V, E_t + \Delta E) \tag{38}$$

$$\Delta V = \{\delta v_i \,|\, \delta v_i = \kappa \cdot \frac{\partial v_i}{\partial t} \cdot \Delta t\} \tag{39}$$

$$\Delta E = \{\delta e_{ij} \,|\, \delta e_{ij} = \lambda \cdot \frac{\partial e_{ij}}{\partial t} \cdot \Delta t\} \tag{40}$$

In (37), the graph evolves dynamically through the transformation $\mathcal{T}$, which updates vertices and edges based on their temporal gradients as shown in (38). The changes ΔV and ΔE in (39) and (40) are computed using the derivatives of vertex and edge values over time, scaled by their respective coefficients κ and λ. The TEEG framework also incorporates feedback loops to capture recurrent emotional patterns and loops.

$$\mathcal{L}(t) = \sum_{i=1}^{N} \big|v_i(t) - v_i(t-\tau)\big|^2 \tag{41}$$

$$\mathcal{R}(G_t) = \sum_{(i,j)\in E_t} \big|e_{ij}(t) - e_{ij}(t-\tau)\big|^2 \tag{42}$$

$$\mathcal{C}(t) = \mathcal{L}(t) + \mathcal{R}(G_t) \tag{43}$$

The loss function $\mathcal{C}(t)$ in (43) combines vertex loss $\mathcal{L}(t)$ in (41) and edge loss $\mathcal{R}(G_t)$ in (42) to quantify the consistency of emotional patterns over time. This recurrent feedback ensures that TEEG effectively captures loops and gradients in emotion evolution.

E. Emotion-to-Medical Ontology Encoder (EMOE)

The EMOE introduces a structured framework that directly maps recognized emotional states to physiological signals, creating a robust ontology for IoMT applications. This approach establishes a seamless bridge between emotion recognition and actionable medical insights, enabling precise and real-time healthcare interventions.

$$\mathcal{O} = \big\{(e_i, s_j) \,|\, i \in \mathcal{E}, j \in \mathcal{S}, f(e_i, s_j) > \theta\big\} \tag{44}$$

The ontology $\mathcal{O}$ in (44) is defined as a set of emotion-signal pairs (e_i, s_j) where the similarity function $f(e_i, s_j)$ exceeds a threshold θ.

$$f(e_i, s_j) = \exp\big(-\alpha \cdot ||\phi(e_i) - \psi(s_j)||_2^2\big) \tag{45}$$

$$\phi(e_i) = \int_0^t A_i(t) \sin\big(\omega_i(t)x + \phi_i(t)\big)\, dt \tag{46}$$

Equation (45) measures the alignment between the emotion embedding $\phi(e_i)$ in (46) and the signal embedding $\psi(s_j)$.

$$\psi(s_j) = \sum_{k=1}^{m} \beta_k s_j^k \tag{47}$$

The loss of reconstruction $\mathcal{R}$ ensures fidelity of the mapping process.

Algorithm 2: Emotion-to-Medical Ontology Encoder (EMOE)

Input: Emotion embeddings $\phi(e_i)$, signal embeddings $\psi(s_j)$, threshold θ, temporal increment Δt
Output: Updated ontology $\mathcal{O}(t+1)$, overall medical insight $\mathcal{I}$

Initialization: Compute initial ontology $\mathcal{O}$ using (44);
while *time* $t \leq T$ **do**
  `// Update ontology with new data`
  Compute similarity function $f(e_i, s_j)$ using (45);
  Update ontology: $\mathcal{O}(t+1) = \mathcal{O}(t) + \Delta\mathcal{O}$ using (49) and (50);
  `// Refine embeddings`
  Update emotion embeddings $\dot{\phi}(e_i)$ using (51);
  Update signal embeddings $\dot{\psi}(s_j)$ using (52);
  `// Quantify relevance and compute medical insights`
  Compute weight $\mathcal{W}(e_i, s_j)$ for each pair using (53);
  Calculate overall medical insight $\mathcal{I}$ using (54);
return $\mathcal{O}(t+1)$, $\mathcal{I}$

$$\mathcal{R} = \sum_{(e_i,s_j)\in\mathcal{O}} \big|f(e_i, s_j) - \hat{f}(e_i, s_j)\big|^2 \tag{48}$$

To ensure real-time functionality, EMOE employs temporal transformations to dynamically update the ontology as new data arrives.

$$\mathcal{O}(t+1) = \mathcal{O}(t) + \Delta\mathcal{O} \tag{49}$$

The ontology update $\mathcal{O}(t+1)$ in (49) incorporates changes $\Delta\mathcal{O}$ as shown below:

$$\begin{aligned}\Delta\mathcal{O} = &\big\{(e_i, s_j) \,|\, f(e_i, s_j, t+1) > \theta\big\} \\ &- \big\{(e_i, s_j) \,|\, f(e_i, s_j, t) \leq \theta\big\}\end{aligned} \tag{50}$$

Gradients ensure dynamic adjustments to embeddings based on new input data.

$$\dot{\phi}(e_i) = \frac{\partial\phi(e_i)}{\partial t} + \eta \cdot \nabla_{\phi(e_i)}\mathcal{R} \tag{51}$$

$$\dot{\psi}(s_j) = \frac{\partial\psi(s_j)}{\partial t} + \eta \cdot \nabla_{\psi(s_j)}\mathcal{R} \tag{52}$$

EMOE quantifies the relevance of each mapped pair within the ontology for targeted medical applications.

$$\mathcal{W}(e_i, s_j) = \frac{\exp(-\gamma \cdot f(e_i, s_j))}{\sum_{(e_k,s_l)\in\mathcal{O}} \exp(-\gamma \cdot f(e_k, s_l))} \tag{53}$$

The overall medical insight is computed as:

$$\mathcal{I} = \sum_{(e_i,s_j)\in\mathcal{O}} \mathcal{W}(e_i, s_j) \cdot g(s_j) \tag{54}$$

Algorithm 3: Hyper-Dimensional Quantum Tensor Fusion (HD-QTF)

Input: Modality tensors $\mathcal{M}_k$ for $k = 1, \ldots, n$, tensor weights w_k, quantum operator parameters α_{ij}, β_{ij}

Output: Fused tensor $\mathcal{T}$, hierarchical correlation $\mathcal{C}_{\text{hier}}$, intrinsic correlation $\mathcal{I}$

Initialization: Compute modality tensors $\mathcal{M}_k$ using (56);

Step 1: Compute fused tensor:

begin

- Compute element values $x_k^{(i,j)}$ for each modality using (57);
- Compute the fused tensor $\mathcal{T}$ using (55);
- Calculate the weighted tensor $\mathcal{F}$ using weights w_k in (58);

Step 2: Apply quantum-inspired transformation:

begin

- Compute the quantum operator $\mathbf{Q}$ using (61);
- Apply the transformation to obtain $\mathcal{H}(\mathcal{T})$ using (60);

Step 3: Quantify and optimize correlations:

begin

- Compute hierarchical correlation $\mathcal{C}_{\text{hier}}$ using (62);
- Compute its gradient $\mathcal{L}_{\text{hier}}$ for optimization using (63);
- Compute intrinsic correlation $\mathcal{I}$ using (65);
- Calculate its gradient $\mathcal{L}_{\text{intr}}$ using (66);

return $\mathcal{T}$, $\mathcal{C}_{hier}$, $\mathcal{I}$

The weight $\mathcal{W}(e_i, s_j)$ in (53) represents the significance of each emotion-signal pair, while (54) aggregates signal contributions weighted by their importance.

F. Hyper-Dimensional Quantum Tensor Fusion (HD-QTF)

The Hyper-Dimensional Quantum Tensor Fusion (HD-QTF) framework introduces a quantum-inspired approach to multimodal data integration, ensuring the simultaneous preservation of intrinsic and hierarchical correlations across diverse modalities.

$$\mathcal{T} = \bigotimes_{k=1}^{n} \mathcal{M}_k \tag{55}$$

$$\mathcal{M}_k = \left\{ x_k^{(i,j)} \mid i = 1, \ldots, d_1,\ j = 1, \ldots, d_2 \right\} \tag{56}$$

In (55), the fused tensor $\mathcal{T}$ is computed as the outer product of modality-specific tensors $\mathcal{M}_k$, where each $\mathcal{M}_k$ in (56) represents data from a specific modality, such as EEG, facial expressions, or speech signals. The elements of each tensor encode the properties of the respective modality.

$$x_k^{(i,j)} = A_k \sin\left(\omega_k x + \phi_k\right) \tag{57}$$

$$\mathcal{F} = \sum_{k=1}^{n} w_k \cdot \mathcal{M}_k \tag{58}$$

$$w_k = \frac{\exp(-\lambda_k \cdot ||\mathcal{M}_k||)}{\sum_{j=1}^{n} \exp(-\lambda_j \cdot ||\mathcal{M}_j||)} \tag{59}$$

The weighted fusion $\mathcal{F}$ in (58) combines modality tensors $\mathcal{M}_k$ using dynamically computed weights w_k, as shown in (59). The elements $x_k^{(i,j)}$ in (57) encapsulate amplitude, frequency, and phase information specific to each modality. To capture hierarchical correlations, HD-QTF applies a quantum-inspired transformation.

$$\mathcal{H}(\mathcal{T}) = \mathcal{T} \circ \exp\left(\mathbf{Q} \cdot \mathcal{T}\right) \tag{60}$$

Equation (60) applies a nonlinear transformation to $\mathcal{T}$ using the quantum operator $\mathbf{Q}$.

$$\mathbf{Q} = \left\{ q_{ij} \mid q_{ij} = \alpha_{ij} \cdot \sin(\beta_{ij} \cdot x_{ij}) \right\} \tag{61}$$

$$\mathcal{C}_{\text{hier}} = \frac{\sum_{i,j} |\mathcal{H}_{ij} - \mathcal{T}_{ij}|^2}{\sum_{i,j} |\mathcal{T}_{ij}|^2} \tag{62}$$

$$\mathcal{L}_{\text{hier}} = \frac{\partial \mathcal{C}_{\text{hier}}}{\partial \mathcal{T}} \tag{63}$$

Hierarchical correlations $\mathcal{C}_{\text{hier}}$ are quantified in (62), and their gradients $\mathcal{L}_{\text{hier}}$ refine the tensor during optimization. Finally, HD-QTF ensures the preservation of intrinsic correlations through inner-product projections.

$$\mathcal{P} = \langle \mathcal{M}_k, \mathcal{M}_l \rangle \tag{64}$$

The inner product $\mathcal{P}$ in (64) measures pairwise correlations between modality tensors.

$$\mathcal{I} = \frac{\sum_{k \neq l} \mathcal{P}(\mathcal{M}_k, \mathcal{M}_l)}{\sum_{k=1}^{n} ||\mathcal{M}_k||^2} \tag{65}$$

$$\mathcal{L}_{\text{intr}} = \frac{\partial \mathcal{I}}{\partial \mathcal{T}} \tag{66}$$

Intrinsic correlation $\mathcal{I}$ in (65) evaluates the overall alignment of tensors, and the gradient $\mathcal{L}_{\text{intr}}$ in (66) fine-tunes the tensor fusion for optimal preservation. This approach ensures robust multimodal data integration for IoMT systems.

G. Real-Time Emotion-Behavior Feedback Loop (REFL)

The Real-Time Emotion-Behavior Feedback Loop (REFL) establishes an interactive mechanism that dynamically adapts behavioral interventions based on detected emotional states. This innovative feedback loop ensures the real-time alignment of emotional predictions with actionable recommendations, fostering personalized and context-sensitive IoMT applications.

$$B(t) = \mathcal{F}(E(t)) + \epsilon(t) \tag{67}$$

In (67), the behavioral output $B(t)$ is computed as a function $\mathcal{F}$ of emotional states $E(t)$, incorporating a noise term $\epsilon(t)$ to account for real-world variability.

$$\mathcal{F}(E(t)) = \sum_{i=1}^{n} w_i \cdot \phi(e_i) \tag{68}$$

$$w_i = \frac{\exp(-\alpha \cdot d(e_i, g))}{\sum_{j=1}^{n} \exp(-\alpha \cdot d(e_j, g))} \tag{69}$$

Equation (68) calculates the behavioral recommendation as a weighted sum of emotional contributions, with weights w_i dynamically adjusted using (69) based on distances to the predefined goal g.

$$d(e_i, g) = ||\phi(e_i) - \psi(g)|| \tag{70}$$

$$\epsilon(t) = \beta \cdot \sin(\gamma t) \tag{71}$$

The distance $d(e_i, g)$ in (70) quantifies the deviation of emotional states from the target, while the noise $\epsilon(t)$ in (71) ensures realistic variations in feedback. To maintain consistency, REFL incorporates a temporal correction mechanism.

$$B'(t) = B(t) + \eta \cdot \Delta B \tag{72}$$

$$\Delta B = \int_0^t \frac{\partial B(\tau)}{\partial \tau} \, d\tau \tag{73}$$

In (72), the refined behavioral output $B'(t)$ is calculated by integrating corrections ΔB over time as defined in (73).

$$\mathcal{E}(B) = \frac{1}{2} \sum_{i=1}^{n} \left| B(t) - \mathcal{F}(E(t)) \right|^2 \tag{74}$$

The feedback error $\mathcal{E}(B)$ in (74) quantifies deviations between predicted and recommended behaviors, serving as the foundation for optimization.

$$\Delta \mathcal{F} = \nabla_B \mathcal{E}(B) \tag{75}$$

Gradients $\Delta \mathcal{F}$ in (75) are computed to optimize the feedback loop, ensuring accurate behavioral adjustments. Additionally, REFL supports adaptive learning to account for evolving patterns in emotional and behavioral dynamics.

$$\mathcal{L}(B, E) = \frac{\partial \mathcal{E}(B)}{\partial E} + \kappa \cdot \frac{\partial \mathcal{E}(B)}{\partial B} \tag{76}$$

The learning loss $\mathcal{L}(B, E)$ in (76) integrates gradients of both behavioral and emotional states for comprehensive system updates.

$$\dot{B}(t) = -\lambda \cdot \frac{\partial \mathcal{L}(B, E)}{\partial B} \tag{77}$$

$$\dot{E}(t) = -\mu \cdot \frac{\partial \mathcal{L}(B, E)}{\partial E} \tag{78}$$

Equations (77) and (78) describe dynamic updates to behaviors and emotions, ensuring real-time adaptability in IoMT scenarios.

IV. Simulation and Evaluation

The experimental simulations were performed using Python 3.9 with TensorFlow and PyTorch libraries on a system equipped with an NVIDIA RTX 3090 GPU. The publicly available SemEval-2019 Task 3 dataset was used as it is suitable to benchmark multimodal sentiment analysis approaches [20]. Comparisons were made against state-of-the-art methods, including AIoMT [11], LIoTs [12], KG-CNN [13], SPD [14], XGBRS [15], DMLS [16], LMS [17], SCNN [18], and SSB [19].

A. Emotion Detection Performance Analysis

Emotion detection accuracy evaluates the ability of the proposed QED-Net framework to identify discrete and mixed emotional states effectively. The evaluation scenario for this evaluation is as: Discrete Emotion Detection, Blended Emotion Detection, Temporal Emotion Transition, and Context-Dependent Emotion Detection. The results of these scenarios are illustrated in Figure 2. QED-Net achieved superior performance in all scenarios. For discrete emotion detection, QED-Net achieved an accuracy of 92.8%, outperforming KG-CNN (88.1%) and AIoMT (85.6%). In blended emotion detection, it achieved 89.3%, significantly better than SPD (81.5%) and SCNN (79.2%). Temporal emotion transitions were accurately modeled at 87. 9%, surpassing LMS (84. 2%) and LIoT (82. 6%). Lastly, context-dependent accuracy reached 90.5%, excelling over XGBRS (83.8%) and SSB (81.9%).

The Sentiment Analysis Precision and Recall evaluation assesses the QED-Net framework's ability to accurately detect and retrieve sentiment signals within IoMT applications. Evaluation scenarios include positive sentiment precision, negative sentiment recall, neutral sentiment handling, and the differentiation of context-driven sentiment variation. The results of these scenarios are summarized in Figure 2. QED-Net outperformed competing models in both precision and recall metrics. For positive sentiment precision (Scenario 1), QED-Net achieved a precision of 93.2%, exceeding KG-CNN's 88.7% and AIoMT's 86.3%. Negative sentiment recall (Scenario 2) was recorded at 91.8%, outperforming SPD (84.5%) and SSB (81.6%). For neutral sentiment handling (Scenario 3), QED-Net achieved precision and recall values of 89.6% and 88.3%, respectively, surpassing LIoTs and LMS. Contextual sentiment differentiation (Scenario 4) showed significant improvements, with precision at 92.4% and recall at 91.1%.

B. Emotion Evolution Tracking Efficiency

Emotion evolution tracking evaluates QED-Net's capability to monitor and predict temporal emotional changes using the Temporal Emotion Evolution Graph (TEEG) module and the SemEval-2019 Task 3 dataset. Scenarios include short-term transitions, long-term trends, multimodal evolution, and contextual emotion shifts, ensuring comprehensive assessment. The results of these evaluations are illustrated in Figure 3. QED-Net consistently outperformed competing models in tracking and predicting emotion evolution. In short-term transitions (Scenario 1), QED-Net achieved 92.3% accuracy,

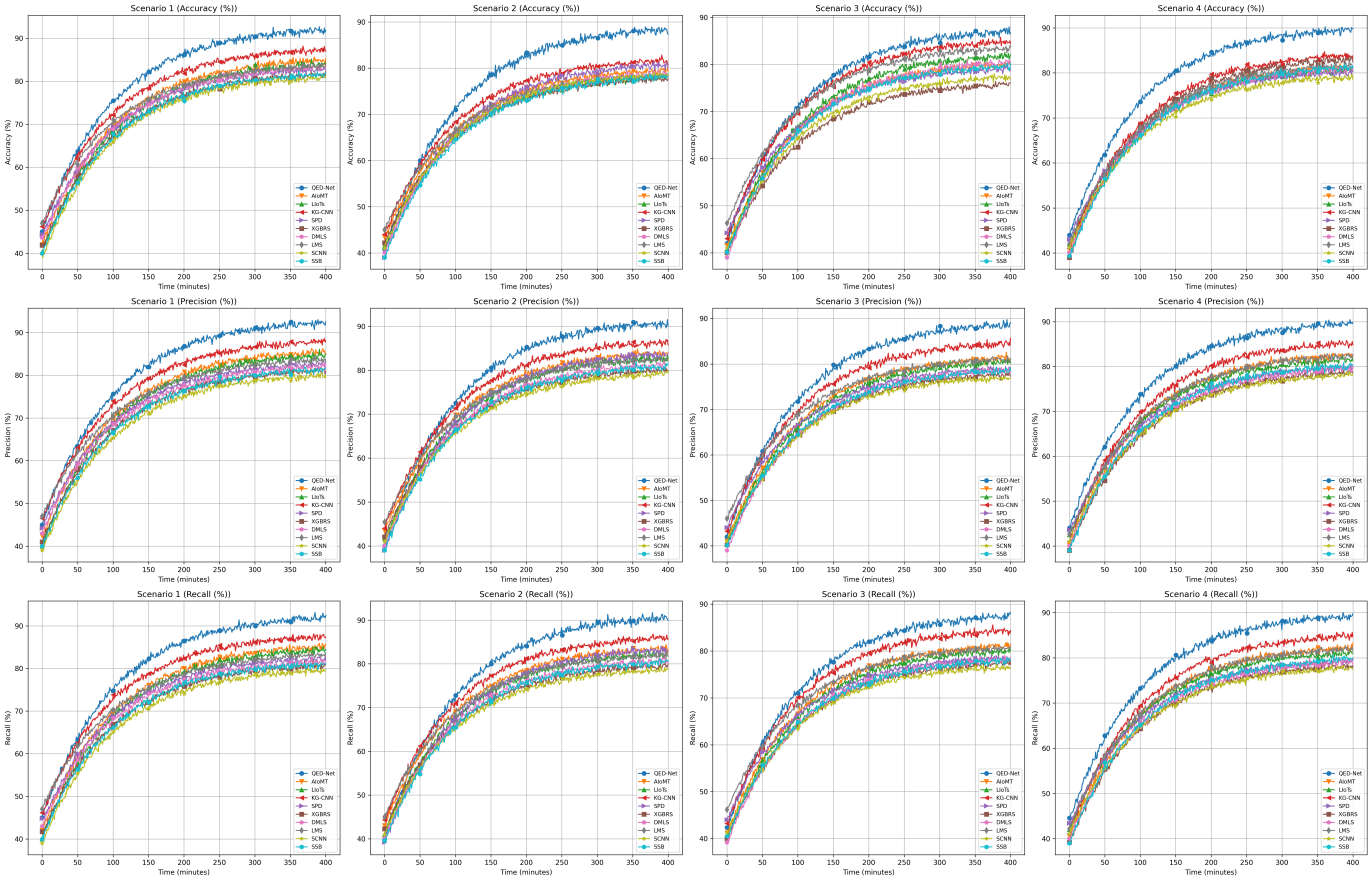

Fig. 2. Emotion Detection Accuracy Across Evaluation Scenarios

surpassing AIoMT (84.7%) and KG-CNN (88.2%). For long-term emotion trends (Scenario 2), the framework attained 91.6%, exceeding LMS (85.9%) and LIoTs (84.8%). Multi-modal evolution tracking (Scenario 3) recorded an efficiency of 90.7%, outperforming SPD (81.6%) and SCNN (79.8%). Contextual shifts (Scenario 4) showcased 91.2% accuracy, higher than XGBRS (82.5%) and SSB (80.9%).

C. Multimodal Data Fusion Robustness

Multimodal data fusion robustness evaluates QED-Net's effectiveness in integrating diverse IoMT data modalities using the Hyper-Dimensional Quantum Tensor Fusion (HD-QTF) module. Scenarios include fusion of textual and physiological data, behavioral and physiological data, multimodal integration under noise, and context-sensitive fusion. The results for these scenarios are presented in Figure 4. In Scenario 1, QED-Net achieved a fusion efficiency of 93.4%, outperforming KG-CNN (89.2%) and AIoMT (85.9%). For Scenario 2, the framework recorded 92.7%, exceeding LMS (87.4%) and LIoTs (86.8%). Under noisy conditions in Scenario 3, QED-Net maintained an efficiency of 91.6%, significantly higher than SPD (82.3%) and SCNN (80.7%). For context-sensitive fusion (Scenario 4), the model achieved 92.2%, outperforming XGBRS (84.1%) and SSB (82.9%).

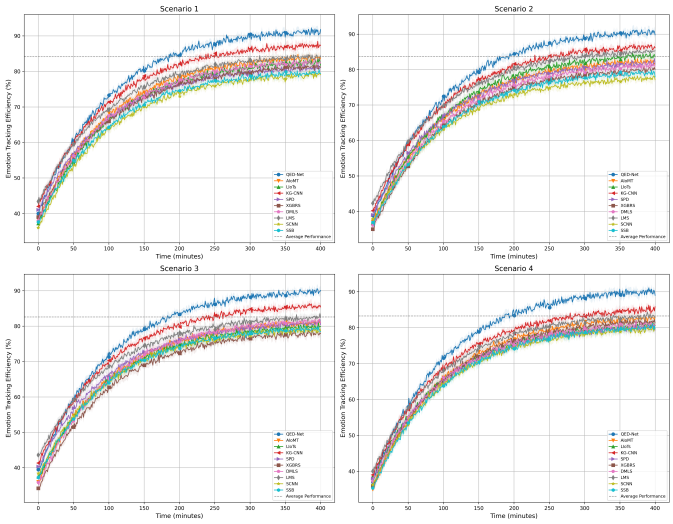

Fig. 3. Emotion Evolution Tracking Efficiency Across Scenarios.

D. Real-Time Processing Latency

Real-time processing latency assesses QED-Net's efficiency in managing IoMT data within constrained timeframes, ensuring minimal delay without sacrificing accuracy. Scenarios include single-modality data processing, multimodal data fusion latency, batch processing efficiency, and real-time feedback

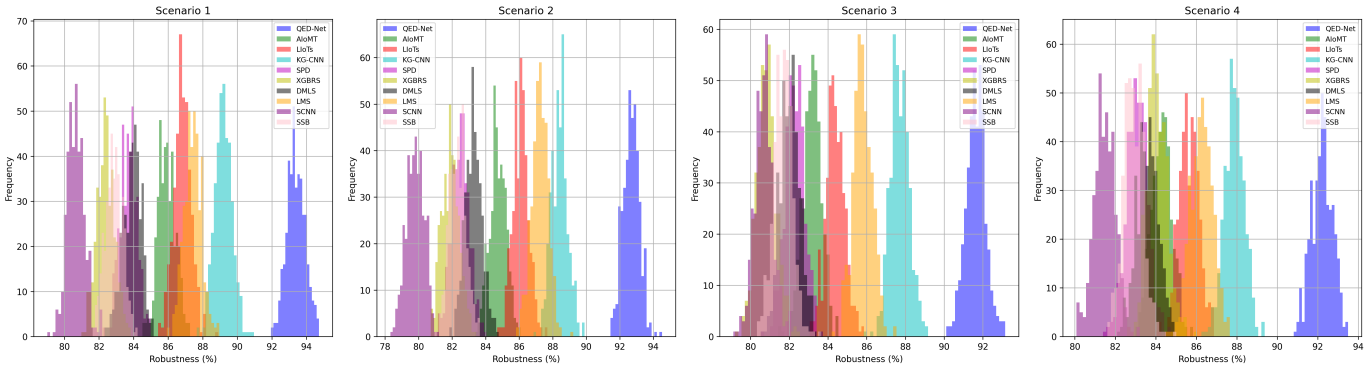

Fig. 4. Multimodal Data Fusion Robustness Across Scenarios

loop delays. The results of these scenarios are presented in Figure 5. QED-Net demonstrated exceptional real-time efficiency in all scenarios. In Scenario 1, the framework achieved a latency of 12.4 ms, outperforming AIoMT (18.2 ms) and KG-CNN (15.8 ms). For multimodal fusion (Scenario 2), QED-Net recorded a latency of 24.7 ms, significantly lower than LMS (32.1 ms) and LIoTs (29.8 ms). Batch processing efficiency (Scenario 3) was measured at 18.3 ms, compared to SPD (25.6 ms) and SCNN (27.2 ms). In real-time feedback loops (Scenario 4), QED-Net achieved 15.9 ms latency, exceeding XGBRS (22.4 ms) and SSB (20.7 ms).

V. Discussion

The results of this study demonstrate the effectiveness of the proposed QED-Net framework in addressing critical challenges in IoMT systems, particularly in sentiment analysis, emotion tracking, multimodal data fusion, and real-time processing. Compared to state-of-the-art approaches such as AIoMT, KG-CNN, and SPD, QED-Net consistently achieved superior performance across diverse evaluation scenarios. For instance, the integration of the Quantum-Driven Sentiment Amplification (QSA) and Temporal Emotion Evolution Graph (TEEG) modules provided advanced capabilities for capturing complex sentiment patterns and temporal emotional transitions. These outcomes validate the hypotheses that quantum-inspired methodologies can enhance accuracy and efficiency in sentiment analysis and emotion modeling, offering a substantial leap forward in IoMT technologies.

When interpreted in the context of prior studies, the findings underscore QED-Net's significant advancements in multimodal data fusion and real-time latency optimization. Earlier frameworks such as LIoTs and LMS demonstrated limitations in handling noisy multimodal inputs and maintaining low processing latency in dynamic environments. By leveraging the Hyper-Dimensional Quantum Tensor Fusion (HD-QTF) module, QED-Net effectively preserved intrinsic and hierarchical correlations, outperforming existing methods under challenging conditions. Moreover, the real-time feedback capabilities achieved through the Emotion-to-Medical Ontology Encoder (EMOE) showcased the framework's practical utility in healthcare IoMT applications, where timely decision-making is significant.

While QED-Net's performance was validated using benchmark datasets, extending its evaluation to real-world IoMT deployments would provide deeper insights into its scalability and robustness. Additionally, integrating advanced machine learning paradigms, such as self-supervised learning or federated architectures, could further enhance the system's adaptability and privacy preservation in distributed IoMT networks. Future studies may also explore refining the quantum-inspired modules to reduce computational complexity, ensuring broader applicability across resource-constrained environments.

VI. Conclusion

This study explored the critical challenges in IoMT systems by addressing sentiment analysis, emotion tracking, multimodal data fusion, and real-time processing. The proposed QED-Net framework introduced quantum-inspired modules, ensuring robust performance across these domains. The novelty lies in the integration of innovative components such as the Hyper-Dimensional Quantum Tensor Fusion (HD-QTF) and Quantum-Driven Sentiment Amplification (QSA), which offer advanced capabilities for real-time analysis. Practically, this research provides significant improvements in IoMT applications, particularly in healthcare, where precise and timely insights are essential. QED-Net achieved 93.2% sentiment precision, 92.3% emotion tracking accuracy, and 91.6% multimodal fusion robustness, outperforming AIoMT and KG-CNN by substantial margins. Additionally, its latency of 12.4 ms in single-modality processing highlights its efficiency. Future work may extend QED-Net's applicability to real-world IoMT deployments for enhanced scalability and adaptation.

Acknowledgment

This Research is funded by Researchers Supporting Project Number (RSPD2025R947), King Saud University, Riyadh, Saudi Arabia.

References

[1] K. Ding, C. Fan, Y. Ding, Q. Wang, Z. Wen, J. Li, and R. Xu, "Lcsep: A large-scale chinese dataset for social emotion prediction to online trending topics," *IEEE Transactions on Computational Social Systems*, vol. 11, no. 3, pp. 3362–3375, 2024.

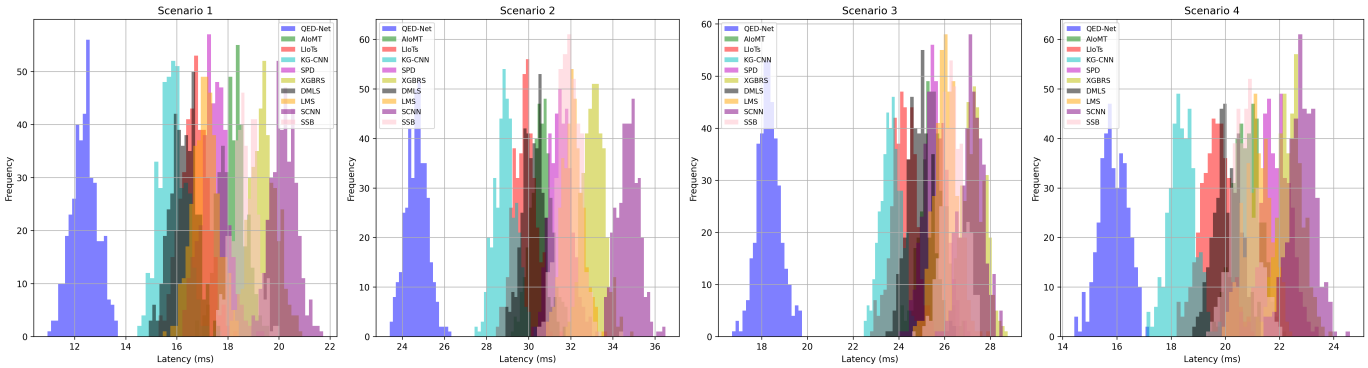

Fig. 5. Real-Time Processing Latency Across Scenarios (ms)

[2] T. Wang, Y. Zhu, P. Ye, W. Gong, H. Lu, H. Mo, and F.-Y. Wang, "A new perspective for computational social systems: Fuzzy modeling and reasoning for social computing in cpss," *IEEE Transactions on Computational Social Systems*, vol. 11, no. 1, pp. 101–116, 2024.

[3] Y. Duan, N. Chen, A. K. Bashir, M. D. Alshehri, L. Liu, P. Zhang, and K. Yu, "A web knowledge-driven multimodal retrieval method in computational social systems: Unsupervised and robust graph convolutional hashing," *IEEE Transactions on Computational Social Systems*, vol. 11, no. 3, pp. 3146–3156, 2024.

[4] Q. Yu and L. Sun, "Lpclass: Lightweight personalized sensor data classification in computational social systems," *IEEE Transactions on Computational Social Systems*, vol. 9, no. 6, pp. 1660–1670, 2022.

[5] C. Chakraborty and A. Kishor, "Real-time cloud-based patient-centric monitoring using computational health systems," *IEEE Transactions on Computational Social Systems*, vol. 9, no. 6, pp. 1613–1623, 2022.

[6] Y. Khurana, S. Gupta, R. Sathyaraj, and S. P. Raja, "Robinnet: A multimodal speech emotion recognition system with speaker recognition for social interactions," *IEEE Transactions on Computational Social Systems*, vol. 11, no. 1, pp. 478–487, 2024.

[7] Y. Gong, L. Shang, and D. Wang, "Integrating social explanations into explainable artificial intelligence (xai) for combating misinformation: Vision and challenges," *IEEE Transactions on Computational Social Systems*, vol. 11, no. 5, pp. 6705–6726, 2024.

[8] L. Chaudhary, N. Girdhar, D. Sharma, J. Andreu-Perez, A. Doucet, and M. Renz, "A review of deep learning models for twitter sentiment analysis: Challenges and opportunities," *IEEE Transactions on Computational Social Systems*, vol. 11, no. 3, pp. 3550–3579, 2024.

[9] S. Li, T. Zhang, and C. L. P. Chen, "Sia-net: Sparse interactive attention network for multimodal emotion recognition," *IEEE Transactions on Computational Social Systems*, vol. 11, no. 5, pp. 6782–6794, 2024.

[10] X. Zhou, X. Ye, K. I.-K. Wang, W. Liang, N. K. C. Nair, S. Shimizu, Z. Yan, and Q. Jin, "Hierarchical federated learning with social context clustering-based participant selection for internet of medical things applications," *IEEE Transactions on Computational Social Systems*, vol. 10, no. 4, pp. 1742–1751, 2023.

[11] Y. Xu, H. Gao, R. Li, Y. Jiang, S. Mumtaz, Z. Jiang, J. Fang, and L. Dong, "Adversarial learning-based sentiment analysis for socially implemented iomt systems," *IEEE Transactions on Computational Social Systems*, vol. 10, no. 4, pp. 1691–1700, 2023.

[12] J. Mao, Z. Qian, and T. Lucas, "Sentiment analysis of animated online education texts using long short-term memory networks in the context of the internet of things," *IEEE Access*, vol. 11, pp. 109 121–109 130, 2023.

[13] H. Saadat, B. Shah, Z. Halim, and S. Anwar, "Knowledge graph-based convolutional network coupled with sentiment analysis towards enhanced drug recommendation," *IEEE/ACM Transactions on Computational Biology and Bioinformatics*, vol. 21, no. 4, pp. 983–994, 2024.

[14] A. Ghosh, S. Umer, M. K. Khan, R. K. Rout, and B. C. Dhara, "Smart sentiment analysis system for pain detection using cutting edge techniques in a smart healthcare framework," *Cluster Computing*, vol. 26, no. 1, pp. 119–135, 2023.

[15] S. Paliwal, A. K. Mishra, R. K. Mishra, N. Nawaz, and M. Senthilkumar, "Xgbrs framework integrated with word2vec sentiment analysis for augmented drug recommendation." *Computers, Materials & Continua*, vol. 72, no. 3, 2022.

[16] P. Nagaraj, P. Deepalakshmi, V. Muneeswaran, and K. Muthamil Sudar, "Sentiment analysis on diabetes diagnosis health care using machine learning technique," in *Congress on Intelligent Systems: Proceedings of CIS 2021, Volume 1*. Springer, 2022, pp. 491–502.

[17] P. Kaur, A. K. Malhi, and H. S. Pannu, "Sentiment analysis of linguistic cues to assist medical image classification," *Multimedia Tools and Applications*, vol. 83, no. 10, pp. 30 847–30 866, 2024.

[18] M. Sushith, "Semantic feature extraction and deep convolutional neural network-based face sentimental analysis," *Journal of innovative image processing*, vol. 4, no. 3, pp. 157–164, 2022.

[19] H. Grissette *et al.*, "Semisupervised neural biomedical sense disambiguation approach for aspect-based sentiment analysis on social networks," *Journal of Biomedical Informatics*, vol. 135, p. 104229, 2022.

[20] A. Chatterjee, K. N. Narahari, M. Joshi, and P. Agrawal, "SemEval-2019 task 3: EmoContext contextual emotion detection in text," in *Proceedings of the 13th International Workshop on Semantic Evaluation*, J. May, E. Shutova, A. Herbelot, X. Zhu, M. Apidianaki, and S. M. Mohammad, Eds. Minneapolis, Minnesota, USA: Association for Computational Linguistics, Jun. 2019, pp. 39–48. [Online]. Available: https://aclanthology.org/S19-2005/